

Properties of Particle Trajectory around a Weakly Magnetized Black Hole

Amritendu Haldar^{*1} and Ritabrata Biswas^{†2}

^{*}Department of Physics, Sripat Singh College, Jiaganj, Murshidabad – 742123, India.

[†] Department of Mathematics, Burdwan University, Burdwan – 713 104, India.

Abstract

In recent years, the dynamics of particles around the black holes surrounded by weak magnetic field is an interesting matter to study. We investigate here the dynamics of charged particles around charged accelerating AdS (Anti-de-Sitter) black hole in the absence and presence of magnetic field by computing *Euler – Lagrange* equations of motion. We further calculate the escape energy, escape velocity for both cases and a comparative analysis being done. Moreover we investigate the center of mass energy of colliding particles for the same. Finally, we compute the effective force acting on the charged particles in the curved background and study its dependence on the radius of black hole graphically.

Keywords : Euler-Lagrange equation; cyclic co-ordinate; escape velocity; center of mass energy and effective force.

1 Introduction

Black Hole (BH hereafter) is the important prediction of General Relativity (GR hereafter). BHs are specified by the curved space-time geometry and bounded by the event horizons. Now a days, the study of dynamics of particles around the BHs in the astrophysical background is found in many literature. Both the particles and photons in the vicinity of the BHs are highly attracted by the strong gravitational pull and as a result the accreted particles cause the gain of mass of the BHs. Again it is also possible that the BHs throw the particles away with high relativistic velocity due to angular momentum barrier. Furthermore the highly energised charged particles may also be escaped from their stable orbits around the BHs due to the collision with other particles and is moved under the influence of the Lorentz force in the electromagnetic fields.

If the gravitational and electromagnetic fields are strong, the motions of the charged particles become in general chaotic and undetermined and so the corresponding orbits become unstable except the inner most stable circular orbit. The weak magnetic field does not affect the geometry of BHs but it may affect the motion of charged particles (Znajek, R. 1976; Blandford, R. D. and Znajek, R. L., 1977). In the experimental point of view (Frolov, V., 2003; Borm, C. V. and Spaans, M., 2013) the magnetic field around the BHs occurs due to existance of plasma may be in the form of an accretion disc or a charged gas cloud (Mckinney, J. C. and Narayan, R., 2007; Dobbie, P. B. et. al. 2008) surrounding the BHs.

Mechanically, when the particles of a system collide with each other, the Center of Mass Energy (CEM hereafter) occurs. Near the event horizon of a BH, the high CEM is produced due to the collision of two particles. The mechanism of collision of two particles falling towards the Kerr BH has been proposed by Banados Silk and West (BSW) (Bandos, M., 2009). Furthermore they also showed that the CEM, in the equatorial plane, may be highest for a fast rotating BH. The BSW mechanism has been investigated for different BHs (Berti, E. et al, 2009; Jacobson, T. and Sotiriou, T. P., 2010; Zaslavskii, O. B., 2010; Wei, S. W. et al, 2010; Patil, M. and Joshi, P. S., 2010, 2011; Harada, T. and Kimura, M., 2011; Grib, A. A. and Pavlov, Yu. V., 2011; Hussian, I., 2012; Sadeghi, J. and Pourhassan, B., 2012; Bambi, C. and Modesto, L., 2013; Tuesunov, A. et al 2013). A general review of the mechanism of collision is viewed in (Harada, T. and Kimura, M., 2014). The CME of the particles at the inner horizon of Kerr BH (Lake, K., 2010), the CEM of the collision of the particles around Kerr- Newmann BH (Wei, S. W. et al, 2010), near the horizon(s) of Kerr-Taup-NUT BH (Liu, C. et al, 2011), cylindrical BH (Said, J. L. and Adami, K.Z., 2011), Plebanski-Demianski BH (Sharif, M. et al, 2013), Kerr-Newmann-Taup-NUT BH (Zakria, A. and Jamil, M., 2015), charged dilaton BH (Pradhan, P., 2015) have been studied.

The study of the dynamics of particles around the BHs in the presence of magnetic field has a special significance in recent time. The authors in (Forlov, V. P. and Shoom, A. A., 2010; Forlov, V. P., 2012; Zahrani, A. A. et al 2013)

¹amritendu.h@gmail.com

²biswas.ritabrata@gmail.com

have investigated the motion of a charged particle near weakly magnetized Schwarzschild BH, in (Nakamura, Y., and Ishizuka, T., 1993; Takahashi, M. and Koyama, H., 2009; Kopacek, O. et al , 2010; Preti, G., 2010; Forlov, V. P. and Krtous, P., 2011; Igata, T., 2011) the authors have analyzed the chaotic motion of a charged particles around Kerr BH near magnetic field. More over in (Pugliese, D. et al , 2011) the authors have studied the circular motion of charged particles around Reissner-Nordstrom BH, in (Majeed, B. et al , 2015) The authors has investigated the dynamics of charged particles around slowly rotating Kerr BH with magnetic field and also in (Jamil, M. et al 2015) the authors has discussed about the dynamics of particles around Schwarzschild BH in the presence of quintessence and magnetic field. Recently, in (Jawad, A., 2016) the authors have investigated the dynamics of particles around a regular BH surrounded by external magnetic field.

Motivated by the previous works, our objective in this letter is to apply the *Euler – Lagrange* equations of motion to study the properties of particle trajectory around the charged accelerating Ads (anti-de-Sitter) BH surrounded by weak magnetic field.

This paper is organized as follows: in next section, we study a charged accelerating AdS BH metric with non-linear electromagnetic source and establish the *Euler – Lagrange* equation of motion radially. In section 3, we analyze the dynamics of charged particles with and without magnetic field around a charged accelerating AdS BH. In section 4, we investigate the CME of two colliding charged particles in the aforesaid conditions and in section 5, we calculate the effective force and explain it with graphical representation. Finally in the last section, we present conclusion of the work.

2 Charged Accelerating AdS (Anti-de-Sitter) Black Holes With Non-linear Electromagnetic Source

A charged accelerating AdS (anti-de-Sitter) BH can be expressed by the metric as (Griffith, J. B. and Podolsky, J., 2006; Hang Liu and Xin-he Meng, 2016):

$$ds^2 = \frac{1}{\Omega^2} \left[f(r)dt^2 - \frac{dr^2}{f(r)} - r^2 \left(\frac{d\theta^2}{g(\theta)} + g(\theta) \sin^2 \theta \frac{d\phi^2}{K^2} \right) \right], \quad (1)$$

where

$$f(r) = (1 - A^2 r^2) \left(1 - \frac{2m}{r} + \frac{q^2}{r^2} + \frac{l^2}{r^2} \right), \quad g(\theta) = 1 + 2m A \cos \theta + q^2 A^2 \cos^2 \theta \quad \text{and} \quad \Omega = 1 + A \cos \theta.$$

The factor Ω determines the conformal infinity of the Ads space. In the above expression m , q , $l = \sqrt{-\frac{\Lambda}{3}}$, (where Λ is cosmological constant) and A represent the mass, electric charge of BHs, Ads radius and magnitude of acceleration of the BHs respectively. The presence of cosmic string may be observed from the variation of the values of $g(\theta)$ at the both poles $\theta_+ = 0$ and $\theta_- = \pi$. Hence

$$K \pm = g(\theta \pm) = 1 \pm 2Am + q^2 A^2 \quad (2)$$

The Lagrangian of a particle of mass m and charge q is expressed by (Zahrani, A. A. et al 2013; Jamil, M. et al 2015):

$$\mathcal{L} = \frac{1}{2} g_{\mu\nu} \frac{dx^\mu}{d\tau} \frac{dx^\nu}{d\tau} + \frac{q}{m} A_\mu \frac{dx^\mu}{d\tau}, \quad (3)$$

where A_μ is the four vector potential for the electromagnetic field.

By employing the Lagrangian dynamics, we now examine the motion of a particle in the background of the BH (1). Here we use the Lagrangian as follows:

$$\mathcal{L}(r) = \frac{1}{\Omega^2} \left[f(r) \dot{t}^2 - \frac{\dot{r}^2}{f(r)} - r^2 \left(\frac{\dot{\theta}^2}{g(\theta)} + g(\theta) \sin^2 \theta \frac{\dot{\phi}^2}{K^2} \right) \right]. \quad (4)$$

The over dot indicates the derivative with respect to proper time. It is evident from the Lagrangian (4) that t , θ and ϕ are cyclic coordinates and hence it leads to corresponding symmetry generators which are also known as Killing vectors. The metric (1) remains invariant under the Killing vector fields X and we obtain:

$$X_0 = \frac{\partial L}{\partial \dot{t}} = 2 \frac{f(r) \dot{t}}{\Omega^2}, \quad (5)$$

$$X_1 = \frac{\partial \mathcal{L}}{\partial \dot{\phi}} = -2 \frac{g(\theta)r^2 \sin^2 \theta \dot{t}}{\Omega^2} \frac{\dot{\phi}}{K^2}, \quad (6)$$

$$X_2 = \cos \phi \frac{\partial \mathcal{L}}{\partial \theta} - \cot \theta \sin \phi \frac{\partial \mathcal{L}}{\partial \dot{\phi}} = -2 \frac{r^2}{\Omega^2} \left(\cos \phi \frac{\dot{\theta}}{g(\theta)} - g(\theta) \sin \theta \cos \theta \sin \phi \frac{\dot{\phi}}{K^2} \right) \quad (7)$$

and

$$X_3 = \sin \phi \frac{\partial \mathcal{L}}{\partial \dot{\theta}} + \cot \theta \cos \phi \frac{\partial \mathcal{L}}{\partial \dot{\phi}} = -2 \frac{r^2}{\Omega^2} \left(\sin \phi \frac{\dot{\theta}}{g(\theta)} + g(\theta) \sin \theta \cos \theta \cos \phi \frac{\dot{\phi}}{K^2} \right) \quad (8)$$

Hence the conservation laws corresponding to the symmetries are depicted as:

$$\text{total energy, } E = \frac{f(r)\dot{t}}{\Omega^2} \text{ and azimuthal angular momentum, } L_z = \frac{g(\theta)r^2 \sin^2 \theta}{\Omega^2} \frac{\dot{\phi}}{K^2}, \quad (9)$$

angular momenta,

$$L_1 = \frac{r^2}{\Omega^2} \left(\cos \phi \frac{\dot{\theta}}{g(\theta)} - \frac{1}{2} g(\theta) \sin 2\theta \sin \phi \frac{\dot{\phi}}{K^2} \right) \text{ and } L_2 = \frac{r^2}{\Omega^2} \left(\sin \phi \frac{\dot{\theta}}{g(\theta)} + \frac{1}{2} g(\theta) \sin 2\theta \cos \phi \frac{\dot{\phi}}{K^2} \right). \quad (10)$$

It is obvious from equations (7), (8) that if the particle which moves in the equatorial plane, X_2 and X_3 become irrelevant.

Here we apply the *Euler – Lagrange* equation of motion for r only and we obtain:

$$\ddot{r} = \frac{1}{2} \left[2rf(r) \left(\frac{\dot{\theta}^2}{g(\theta)} + g(\theta) \sin^2 \theta \frac{\dot{\phi}^2}{K^2} \right) - f(r)f'(r)\dot{t}^2 - \dot{r}^2 \frac{f'(r)}{f(r)} \right], \quad (11)$$

where $f(r)$, \dot{t} and $\dot{\phi}$ are obtained from equation (9).

3 Dynamics of Charged Particles:

3.1 In the Absence of Magnetic Field:

The constant of motion for the charged particle in the absence of magnetic field is given by equation (9). The particle is associated with the total specific angular momentum as [?, ?]:

$$L^2 \equiv r^4 \dot{\theta}^2 + \frac{L_z^2 \Omega^2 K^4}{g(\theta)^2 \sin^2 \theta} = r^2 v_{\perp}^2 + \frac{L_z^2 \Omega^2 K^4}{g(\theta)^2 \sin^2 \theta}, \quad (12)$$

Applying the normalization condition for four-velocity, we calculate \dot{r}^2 from equation (4) as:

$$\dot{r}^2 = f(r)^2 \dot{t}^2 - f(r) \left[\Omega^2 + \frac{r^2 \dot{\theta}^2}{g(\theta)} + g(\theta) r^2 \sin^2 \theta \frac{\dot{\phi}^2}{K^2} \right]. \quad (13)$$

Since we assume the system is spherically symmetric, all $\theta = \text{constant}$ planes will be equivalent to the equatorial plane for which $\theta = \frac{\pi}{2}$ and hence from *eq* (13) we have

$$\dot{r}^2 = E^2 - f(r) \left[1 + \frac{L_z^2 K^2}{r^2} \right]. \quad (14)$$

Again if we consider the orbit of the particle through which it is moving is circular, then the equation (14) reduces to

$$E^2 = f(r) \left[1 + \frac{L_z^2 K^2}{r^2} \right]. \quad (15)$$

and it is equivalent to the effective potential $U_{\text{eff}}(r)$ of that particle. Hence equation (15) shows that the total energy and / or the effective potential will vanish at the horizon(s).

The critical azimuthal angular momentum of a particle that follows a particular orbit where the effective potential is extremum (i.e., maximum or minimum) and it is expressed as:

$$L_z^2 = \frac{g(\theta)}{K^2} \left(\frac{mr - q^2 + A^2mr^3 - A^2r^4 + \frac{r^4}{l^2} - 2\frac{A^2r^6}{l^2}}{1 + A^2mr - A^2q^2 - 3\frac{m}{r} + 2\frac{q^2}{r^2} + \frac{A^2r^2}{l^2}} \right). \quad (16)$$

Hence the energy of the particle would be

$$E^2 = \frac{f(r)^2}{1 + A^2mr - A^2q^2 - 3\frac{m}{r} + 2\frac{q^2}{r^2} + \frac{A^2r^2}{l^2}}. \quad (17)$$

After collision, the energy of the particle takes the form as:

$$E_c^2 = f(r) \left[1 + \frac{(L_zK + rv_{\perp})^2}{r^2} \right]. \quad (18)$$

So comparing between the eq^n s (17) and (18) we infer that the energy after collision is grater than that of the total energy before collision as the extra term rv_{\perp} is present in eq^n (18) and which is obvious due to the collision. In this expression v_{\perp} is the minimum velocity of the particle required to escape from ISCO and is given as:

$$v_{\perp} = \sqrt{\frac{E_c^2 - f(r)}{f(r)}} - \frac{L_zK}{r\sqrt{g(\theta)}}. \quad (19)$$

3.2 In the Presence of Magnetic Field

If we consider an axially symmetric magnetic field with strength B around the BH, the conservation laws (9) for the charged particle take the form as:

$$E = \frac{f(r)\dot{t}}{\Omega^2} \quad \text{and} \quad L_z = \frac{g(\theta)r^2\sin^2\theta}{\Omega^2} \frac{(\dot{\phi} + B)}{K^2}, \quad (20)$$

The equation of motion of the charged particle in this case is of the same form as equation (11) where $f(r)$, \dot{t} and $\dot{\phi}$ are obtained from eq^n (20).

From eq^n (4) and (20) we have the energy and the corresponding effective potential as:

$$E^2 = \dot{r}^2 + f(r) \frac{r^2\dot{\theta}^2}{g(\theta)} + f(r) \left[\Omega^2 + g(\theta)r^2\sin^2\theta \frac{1}{K^2} \left(\frac{L_z\Omega^2K^2}{g(\theta)r^2\sin^2\theta} - B \right)^2 \right] \quad (21)$$

and

$$U_{eff}(r) = f(r) \left[\Omega^2 + g(\theta)r^2\sin^2\theta \frac{1}{K^2} \left(\frac{L_z\Omega^2K^2}{g(\theta)r^2\sin^2\theta} - B \right)^2 \right]. \quad (22)$$

For the condition as applied in equation (13), we have from equation (21) and (22) that

$$E^2 = \dot{r}^2 + f(r) \left[1 + \frac{r^2}{K^2} \left(\frac{L_zK^2}{r^2} - B \right)^2 \right] \quad (23)$$

and

$$U_{eff}(r) = f(r) \left[1 + \frac{r^2}{K^2} \left(\frac{L_zK^2}{r^2} - B \right)^2 \right]. \quad (24)$$

In order to integrate the dynamical equations, we need to make these equations dimensionless. We use the following transformation relations (Jamil, M. et al 2015; Hussain, S. et al 2014; Hsu, S. D. H., 2004) as:

$$2m = r_d, \quad \tau = \sigma r_d, \quad r = \rho r_d, \quad L_z = \ell r_d, \quad q = \alpha r_d, \quad B = b r_d, \quad l = s r_d \quad \text{and} \quad a = A r_d. \quad (25)$$

Using these relations (23), the equation (11), (21) and (22) acquire the form as:

$$\ddot{\rho} = \frac{1}{2} \left[2\rho f(\rho) \left(\frac{\dot{\theta}^2}{g(\theta)} + g(\theta) \sin^2 \theta \frac{\dot{\phi}^2}{K^2} \right) - f(\rho) f'(\rho) \dot{t}^2 - \frac{\dot{\rho}^2 f'(\rho)}{f(\rho)} \right],$$

$$E^2 = \dot{\rho}^2 + f(\rho) \frac{\rho^2 \dot{\theta}^2}{g(\theta)} + f(\rho) \left[\Omega^2 + g(\theta) \rho^2 \sin^2 \theta \frac{1}{K^2} \left(\frac{\ell \Omega^2 K^2}{g(\theta) \rho^2 \sin^2 \theta} - b \right)^2 \right]$$

and

$$U_{eff}(\rho) = f(\rho) \left[\Omega^2 + g(\theta) \rho^2 \sin^2 \theta \frac{1}{K^2} \left(\frac{\ell \Omega^2 K^2}{g(\theta) \rho^2 \sin^2 \theta} - b \right)^2 \right], \quad (26)$$

where

$$f(\rho) = (1 - a^2 \rho^2) \left(1 - \frac{1}{\rho} + \frac{\alpha^2}{\rho^2} + \frac{\rho^2}{s^2} \right) \text{ and } \Omega = 1 + a \rho \cos \theta. \quad (27)$$

After collision, for $\theta = \frac{\pi}{2}$ and constant ρ the energy given in eqⁿ (26) reduces to

$$E_c^2 = f(\rho) \left[1 + \frac{\rho^2}{K^2} \left(\frac{\ell K^2 + \rho v_{\perp}}{\rho^2} - b \right)^2 \right]. \quad (28)$$

Hence the escape velocity of the charged particle is expressed as:

$$v_{\perp} = K \sqrt{\frac{E_c^2 - f(\rho)}{f(\rho)}} - \frac{\ell K^2}{\rho} + \rho b. \quad (29)$$

We have plotted the variation of escape velocity v_{\perp} of the particle with respect to the radius r of the BH for different values of q, l, K, b, L_z and E_c in Fig- (1a – 1e).

In Fig-1a, we vary q and l simultaneously keeping K, b, L_z , and E_c are fixed and we notice that with increase of q and l , for same r , the escape velocity v_{\perp} decreases. If r is small enough v_{\perp} has a negative value which depicts no physical particle can escape from so near points of a compact object considered here. But once distance from the center of the gravitating object is high we can have an escape velocity which will increase first steeply with the increment of r and latter the rate of increment will be reduced. However the value is ever increasing with r . If we increase q and l keeping all the other parameters constant, the curves stays of the same nature only except the fact that they are amplified. This means for a higher charge, escape velocity is lower. So is for the higher space time curvature, i.e., higher the curvature lower is the escape velocity. This phenomenon is quite obvious as whenever the central engine is attracting gravitationally and electrically it is more hard for the particle to escape from such an object. Besides, if the curvature is high, higher velocity is required.

In Fig-1b, we change the values of K by fixing the other parameters and we find that with increase of K , the particle escapes from higher values of r but for same r , the escape velocity v_{\perp} increases. As we vary K only again for low r we see unphysical escape velocity. With r escape velocity increases. For low r , low K a high v_{\perp} will be required. For high r , low K , the v_{\perp} required is low. For every two K_{low} and K_{high} curves there is a point r_{crit} where the system needs same escape velocity. This is due to the quadratic nature of K in the expression of v_{\perp} in equation (28).

We vary L_z keeping the parameters q, l, K, b , and E_c are unchanged in Fig-1c and we observed that its nature is similar as Fig-1b. Here we noticed that with increase of L_z , the particle escapes from higher values of r but for same r , the escape velocity v_{\perp} decreases.

Fig-1d and Fig-1e have the similar nature. One is plotted by varying the strength of magnetic field b and other with escape energy E_c . We observe from the figures that for higher strength of magnetic field as well as escape energy the escape velocity of the particle is also higher. Hence we conclude that the magnetic field which escape the particle from the vicinity of the BH plays an important role in transfer mechanism of energy.

Fig.-1a

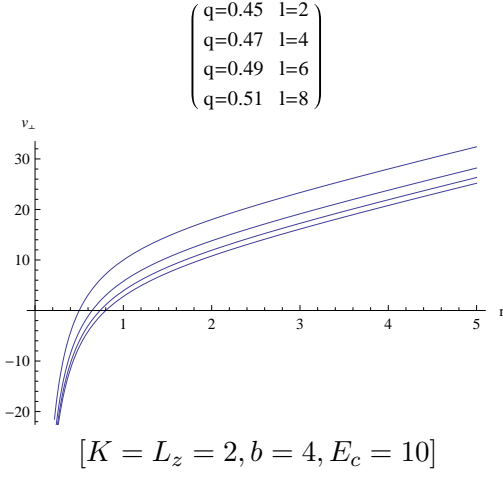


Fig.-1b

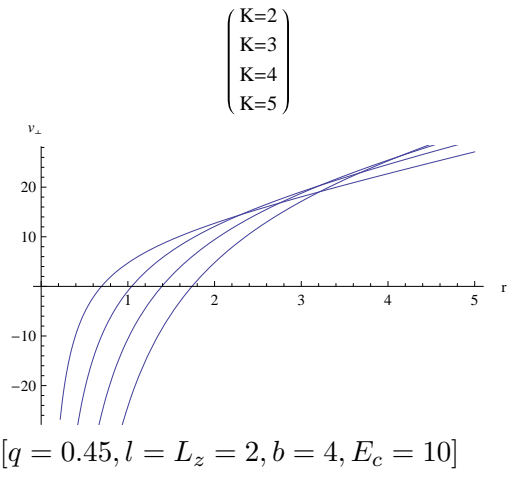


Fig-1a represents the variation of escape velocity v_{\perp} with respect to r keeping K , L_z and b are fixed, with varying q and l ,

Fig-1b represents the variation of escape velocity v_{\perp} with respect to r keeping q , l , L_z and b are fixed with varying K ,

Fig.-1c

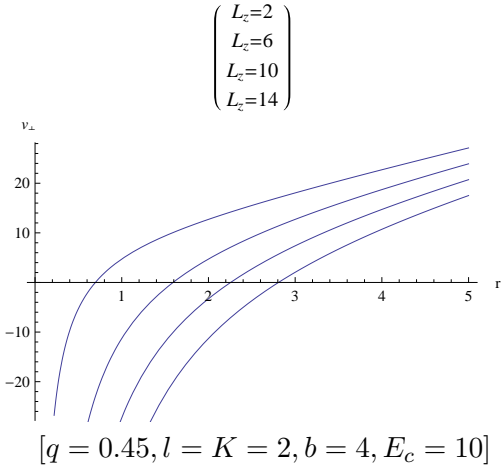


Fig.-1d

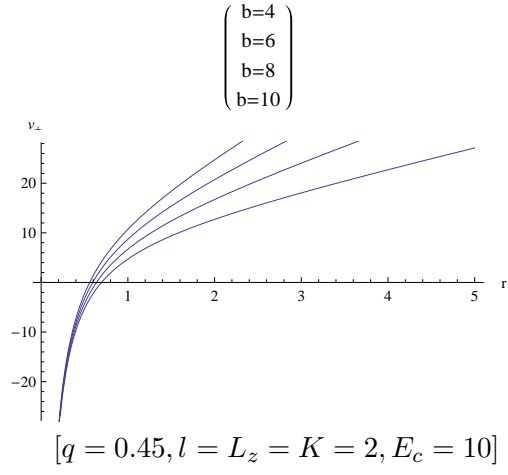


Fig-1c represents the variation of escape velocity v_{\perp} with respect to r keeping q , l , K and b are fixed with varying L_z ,

Fig-1d represents the variation of escape velocity v_{\perp} with respect to r keeping q , l , L_z and K are fixed with varying b ,

We have drawn the curves of effective potential U_{eff} of the particle corresponding to circular orbits with respect to radius r of BH for different values of q , l , K , b , and L_z in Fig- (2a – 2d). We observe a similar feature that there is a minimum value of U_{eff} at r lying between 1 and 2. Initially U_{eff} decreases very sharply (almost straight down) with increases of r and gets negative value when r exceeds the value about 1 and it reaches to a minimum value. Further increases of r , U_{eff} increases to nearly zero and then rapidly decreases.

In Fig-2a, it is found that U_{eff} gets nearly zero value at about $r = 3$ for all the variation of q and l . But Fig-(2b – 2d) show that U_{eff} reaches nearly zero value for different values of r . Due to increase of corresponding parameters, the values of r where U_{eff} reaches nearly zero value also increase.

Fig.-1e

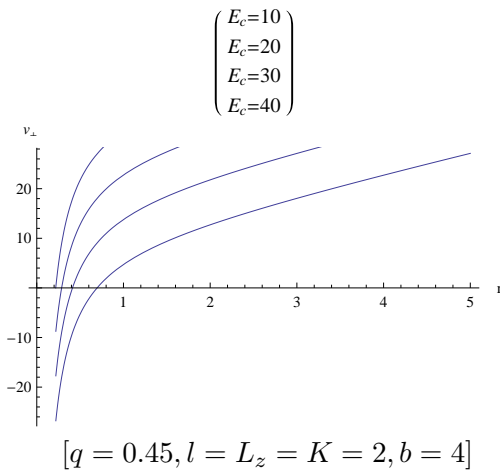
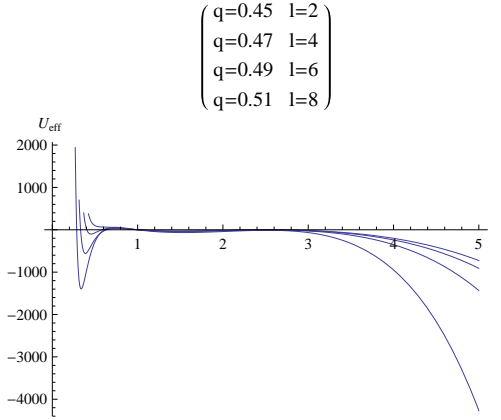


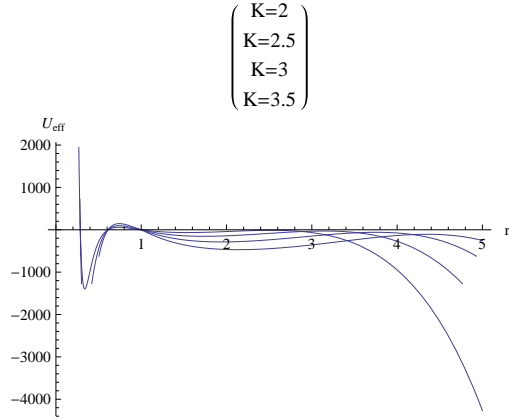
Fig-1e represents the variation of escape velocity v_{\perp} with respect to r keeping K, L_z, q, l and b are fixed, with varying E_c .

Fig.-2a



$$[L_z = 10, K = 2, b = 6]$$

Fig.-2b

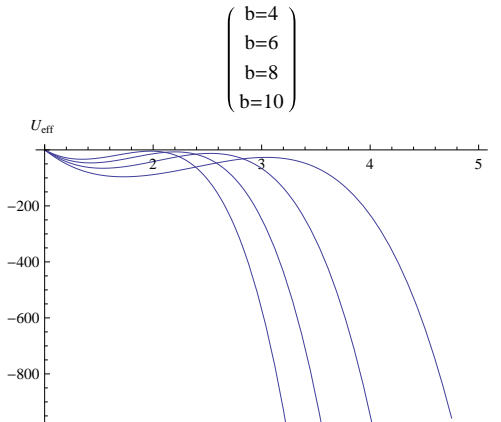


$$[q = 0.45, l = 2, L_z = 10, b = 6]$$

Fig-2a represents the variation of effective potential U_{eff} with respect to r keeping K , L_z and b are fixed, with varying q and l .

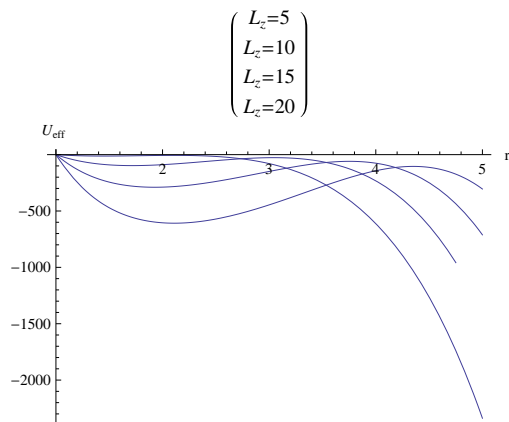
Fig-2b represents the variation of effective potential U_{eff} with respect to r keeping q , l , L_z and b are fixed with varying K .

Fig.-2c



$$[q = 0.45, l = K = 2 \text{ and } L_z = 10]$$

Fig.-2d



$$[q = 0.45, l = K = 2 \text{ and } b = 4]$$

Fig-2c represents the variation of effective potential U_{eff} with respect to r keeping q , l , L_z and K are fixed with varying b .

Fig-2d represents the variation of effective potential U_{eff} with respect to r keeping q , l , K and b are fixed with varying L_z .

4 Center of Mass Energy of the Colliding Charged Particles

The CME of the colliding particles is expressed as [?]:

$$E_{CME} = \sqrt{2}m_o (1 - g_{\mu\nu}u^\mu u^\nu)^{\frac{1}{2}}, \quad (30)$$

where m_o is the mass and u^μ is the 4-velocity of each particles respectively.

4.1 In the Absence of Magnetic Field

Applying eq^n (9) in eq^n (30), we obtain

$$E_{CME} = \sqrt{2}m_o \frac{L_z}{r} (1 - K^2)^{\frac{1}{2}} \simeq \sqrt{2}m_o \frac{L_z}{r} \left(1 - \frac{K^2}{2}\right), \quad (31)$$

4.2 In the Presence of Magnetic Field

Applying eq^n (20) in eq^n (31), we obtain

$$E_{CME} = \sqrt{2}m_o \frac{L_z}{r} \left(1 - K^2 - \frac{r^4 B^2}{L_z^2} + 2\frac{r^4 B}{L_z}\right)^{\frac{1}{2}} \simeq \sqrt{2}m_o \frac{L_z}{r} \left(1 - \frac{K^2}{2} - \frac{r^4 B^2}{2L_z^2} + \frac{r^4 B}{L_z}\right), \quad (32)$$

It is evident from eq^n s (31) and (32) that the CEM of the charged particles with and without magnetic field do not change at horizon(s).

5 Effective Force

The effective force acting on the charged particles in the flat background normally measured by the Lorentz force but in the curved background it may be determined as follows

$$F_{eff} = -\frac{1}{2} \frac{dU_{eff}}{dr} = a^2 r \left(1 - \frac{1}{r} + \frac{\alpha^2}{r^2} + \frac{r^2}{s^2}\right) \left[1 + \frac{r^2}{K^2} \left(\frac{\ell K^2}{r^2} - b\right)^2\right] - (1 - a^2 r^2) \left(\frac{1}{2r^2} - \frac{\alpha^2}{r^3} + \frac{r}{s^2}\right) \left[1 + \frac{r^2}{K^2} \left(\frac{\ell K^2}{r^2} - b\right)^2\right] + 4\frac{\ell}{r^2} (1 - a^2 r^2) \left(1 - \frac{1}{r} + \frac{\alpha^2}{r^2} + \frac{r^2}{s^2}\right) \left(\frac{\ell K^2}{r^2} - b\right). \quad (33)$$

We have plotted here the graphs of effective force f_{eff} acting on the charged particle vs the radius r of BH for different values of q, l, K, b , and L_z in Fig- (3a – 3d). We observe from all the graphs that for $r = 0.3$ f_{eff} has very high value, further very small increases of r , f_{eff} decreases sharply and reaches a minimum value at $r = 0.4$. f_{eff} acquires zero value i.e., constant effective potential at about $r = 0.6$. Fig-3a and Fig-3c are in similar nature. Both the graphs show for higher values of q and l (Fig-3a) and b (Fig-3c), f_{eff} increases more rapidly with increases of r . Again surprisingly the feature of Fig-3b and Fig-3d are similar. Here we vary K and L_z respectively. Both these curves show f_{eff} reaches to Positive value within the range of r about 0.6 to 1.4. For higher values of K and L_z the peak value of f_{eff} is also high. Beyond $r = 1.4$, f_{eff} decreases slightly and then increases rapidly with increases of r this increasing is higher for higher values of K and L_z respectively.

6 Conclusion

In our study, we investigate the dynamic of charged particles around charged accelerating Ads (anti-de-Sitter) black hole in the absence and presence of magnetic field by computing *Euler – Lagrange* equation of motion for radial component only. First of all we choose the charged accelerating Ads (anti-de Sitter) BH with non-linear electromagnetic source and analysis the effective potential, escape energy and therefore escape velocity in the absence and presence of magnetic field. We analysis the dependence of that physical quantities on the radius of BH graphically. We observe from Fig-1a – 1e that the escape velocity of the charged particle increases with increase of the radius of BH as expected. But higher values of charge, Ads radius (Fig-1a), magnetic field (Fig-1d) and escape energy (Fig-1e) the escape velocity for same radius decreases. Whereas the escape velocity for same radius decreases initially for higher values of azimuthal angular momentum (Fig-1b) and cosmic spring constant (Fig-1c). But after a certain range of radius the escape velocity increases for for higher values of azimuthal angular momentum (Fig-1b) and cosmic spring constant (Fig-1c). We observe from Fig-1d and Fig-1e that for higher strength of magnetic field as well as escape energy the escape velocity of the particle is also higher. Hence we conclude that the magnetic field which escape the particle from the vicinity of the BH plays an important role in transfer mechanism of energy. The variation of effective potential with radius of BH is studied in Fig-2a – 2d. All these graph show that there is a minimum negative value when radius is very small. May be this is a stable circular orbit. There are also may exist many stable circular orbits. Moreover we investigate the

Fig.-3a

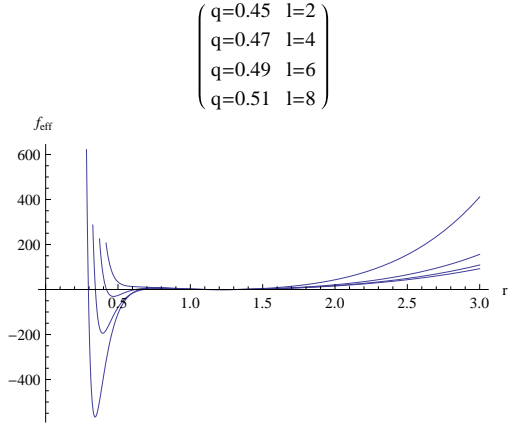
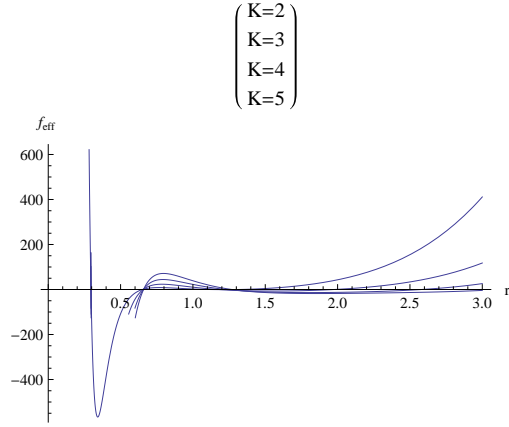


Fig.-3b



$$[L_z = K = 2, b = 4]$$

$$[q = 0.45, l = L_z = 2, b = 4]$$

Fig-3a represents the variation of effective force f_{eff} with respect to r keeping K , L_z and b are fixed, with varying q and l .

Fig-3b represents the variation of effective force f_{eff} with respect to r keeping q , l , L_z and b are fixed with varying K .

Fig.-3c

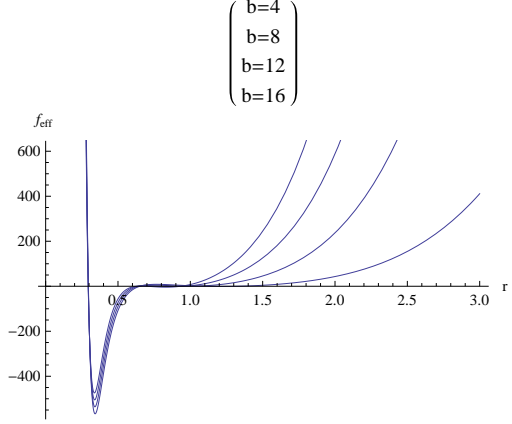
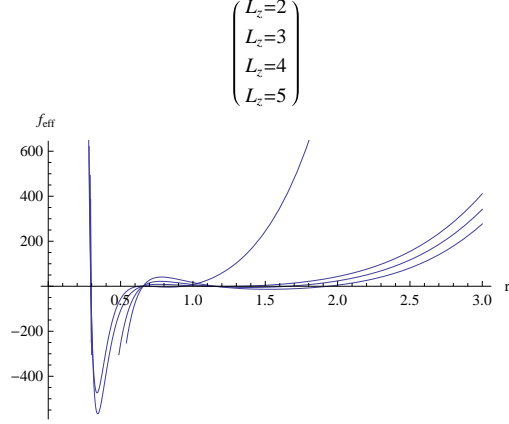


Fig.-3d



$$[q = 0.45, l = L_z = K = 2]$$

$$[q = 0.45, l = K = 2, b = 4]$$

Fig-3c represents the variation of effective force f_{eff} with respect to r keeping q , l , L_z and K are fixed with varying b .

Fig-3d represents the variation of effective force f_{eff} with respect to r keeping q , l , K and b are fixed with varying L_z .

CME of two colliding particles with and without magnetic field. Finally, we calculate the effective force acting on the charged particles in the curved background and examine its dependence on the radius of black hole graphically. We find there is a minimum negative value of effective force at very small radius of BH and then it reaches to zero, stay within few range of the radius for different values of charge and Ads radius (Fig-3a) and magnetic field Fig-3c). Again for different values of cosmic spring constant (Fig-3b) and azimuthal angular momentum (Fig-3d) it reaches to a positive

value whose peak value is higher for higher values cosmic spring constant and azimuthal angular momentum separately.

Acknowledgment: AH wishes to thank the Department of Mathematics, the University of Burdwan for the research facilities provided during the work. RB thanks IUCAA, Pune, India for Visiting Associateship. **References:**

AH wishes to thank the Department of Mathematics, the University of Burdwan for the research facilities provided during the work. RB thanks IUCAA, Pune, India for Visiting Associateship. Bambi, C. and Modesto, L. :-*Phys. Lett. B* **721**, 329 (2013).

Bandos, M., Silk, J. and West, S. M. :-*Phys. Rev. Lett.* **103**, 111102 (2009).
 Berti, E., Cardoso, V., Gualtieri, L., Pretorius, F. and Sperhake, U. :-*Phys. Rev. Lett.* **103**, 239001 (2009).
 Blandford, R. D. and Znajek, R. L. :-*Mon. Not. R. Astron. Soc.* 179,433 (1977).
 Borm, C. V. and Spaans, M. :-*Astron. Astrophys. L* **9** 553 (2013).
 Dobbie, P. B., Kuncic, Z., Bicknell, G. V. and Salmeron, R. :-*Proceeding of IAU Symposium 259 Galaxies* (Tentefire, 2008).
 Frolov, V., The Galactic Black Hole, eds. by Falcke, H., Hehl, F. H. IoP (2003).
 Forlov, V. P. and Shoom, A. A. :-*Phys. Rev. D* **82**, 084034 (2010).
 Forlov, V. P. and Krtous, P. :-*Phys. Rev. D* **83**, 024016 (2011).
 Forlov, V. P. :-*Phys. Rev. D* **85**, 024020 (2012).
 Grib, A. A. and Pavlov, Yu. V. :-*Astropart. Phys.* **34**, 581 (2011).
 Griffith, J. B. and Podolsky, J. :-*A new look at the plebanski-demianski family of solutions*, *Int. J. Mod. Phys. D* **15**, 335-370 (2006).
 Hang Liu and Xin-he Meng :- *arXiv: 1607.00496*, [gr-qc] (2016).
 Harada, T. and Kimura, M. :-*Phys. Rev. D* **83**, 024002 (2011).
 Harada, T. and Kimura, M. :-*Classical Quantum Gravity* **31**, 243001 (2014).
 Hsu, S. D. H. :-*Phys. Lett. B* **594**, 13 (2004).
 Hussain, I. :-*Mod. Phys. Lett. A* **27**, 1250017 (2012).
 Hussain, S., Hussain, I. and Jamil, M. :-*Eur. Phys. J. C* **74**, 3210 (2014).
 Igata, T., Koike, T. and Ishihara, H. :-*Phys. Rev. D* **83**, 065027 (2011).
 Jamil, M., Hussain, S. and Majeed, B. :-*Eur. Phys. J. C* **75**, 24 (2015).
 Jawad, A., Ali, F., Jamil, M. and Debnath, U. :-*arXiv 1610.07411*, [gr-qc] (2016).
 Kopacek, O., Kovar, J., Karas, V. and Stuchlik, Z. :-*AIP Conf. Proc.* **1283**, 278 (2010).
 Lake, K. :-*Phys. Rev. Lett.* **104**, 211102 (2010).
 Liu, C., Chen, S., Ding, C. and Jing, J. :-*Phys. Lett. B* **701**, 285 (2011).
 Majeed, B., Hussain, S. and Jamil, M. :-*Advances in High Energy Physics 2015*, 6712559 (2015).
 McKinney, J. C. and Narayan, R. :-*Mon. Not. R. Astron. Soc.* 375, 523 (2007).
 Nakamura, Y., and Ishizuka, T. :-*Astrophys. Space Sci.* **210**, 105 (1993).
 Patil, M. and Joshi, P. S. :-*Phys. Rev. D* **82**, 104049 (2010).
 Patil, M. and Joshi, P. S. :-*Classical Quantum Gravity* **28**, 235012 (2011).
 Pradhan, P. :-*Astropart. Phys.* **62**, 217 (2015).
 Preti, G. :-*Phys. Rev. D* **81**, 024008 (2010).
 Pugliese, D., Quevedo, H. and Rufini, R. :-*Phys. Rev. D* **83**, 104052 (2011).
 Said, J. L. and Adami, K.Z. :-*Phys. Rev. D* **83**, 104047 (2011).
 Sadeghi, J. and Pourhassan, B. :-*Eur. Phys. J. C* **72**, 1984 (2012).
 Sharif, M., Haider, N. and Theor, J. :-*Exp. Phys.* **117**, 78 (2013).
 Takahashi, M. and Koyama, H. :-*Astrophys. J* **693**, 472 (2009).
 Tuesunov, A., Kolo.s, M., Abdujabbarov, A. Ahmedov, B. and Syuchlik, Z. :-*Phys. Rev. D* **88**, 124001 (2013).
 Zakria, A. and Jamil, M. :-*JHEP* **147**, 1505 (2015).
 Wei, S. W., Liu, Y. X. Guo, H. and Fu, C. E. :-*Phys. Rev. D* **82**, 103005 (2010).
 Wei, S. W., Liu, Y.X., Li, H.T. and Chen, F. W. :-*JHEP* **12**, 066 (2010).
 Zahrani, A. A., Frolov, V. P. and Shoom, A. A. :-*Phys. Rev. D* **87**, 084043 (2013).
 Zaslavskii, O. B. :-*JETP Lett.* **92**, 571 (2010).

Znajek, R. :- *Nature* 262, 270 (1976).